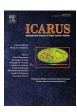


Contents lists available at ScienceDirect

Icarus

journal homepage: www.elsevier.com/locate/icarus



Atmospheric structure and helium abundance on Saturn from Cassini/UVIS and CIRS observations



T.T. Koskinen^{a,*}, S. Guerlet^b

- ^a Lunar and Planetary Laboratory, University of Arizona, 1629 E. University Blvd., Tucson, AZ 85721, USA
- b LMD/IPSL, Sorbonne Universités, UPMC Univ Paris 06, ENS, PSL Research University, École polytechnique, Université Paris Saclay, CNRS, Paris, France

ARTICLE INFO

Article history: Received 12 September 2017 Revised 11 January 2018 Accepted 14 February 2018 Available online 16 February 2018

Keywords: Saturn Occultations Infrared observations Atmospheres Structure

ABSTRACT

We combine measurements from stellar occultations observed by the Cassini Ultraviolet Imaging Spectrograph (UVIS) and limb scans observed by the Composite Infrared Spectrometer (CIRS) to create empirical atmospheric structure models for Saturn corresponding to the locations probed by the occultations. The results cover multiple locations at low to mid-latitudes between the spring of 2005 and the fall of 2015. We connect the temperature-pressure (T-P) profiles retrieved from the CIRS limb scans in the stratosphere to the T-P profiles in the thermosphere retrieved from the UVIS occultations. We calculate the altitudes corresponding to the pressure levels in each case based on our best fit composition model that includes H_2 , H_4 , CH_4 and upper limits on H. We match the altitude structure to the density profile in the thermosphere that is retrieved from the occultations. Our models depend on the abundance of helium and we derive a volume mixing ratio of $11 \pm 2\%$ for helium in the lower atmosphere based on a statistical analysis of the values derived for 32 different occultation locations. We also derive the mean temperature and methane profiles in the upper atmosphere and constrain their variability. Our results are consistent with enhanced heating at the polar auroral region and a dynamically active upper atmosphere.

 $\ensuremath{\mathbb{C}}$ 2018 Elsevier Inc. All rights reserved.

1. Introduction

The Cassini orbiter studied the Saturn system from its orbit insertion in 2004 until the final plunge into Saturn's atmosphere in the fall of 2017. More than a decade of Cassini observations provide unprecedented constraints on atmospheric structure and seasonal change on Saturn. For example, observations of thermal infrared emissions by the Composite Infrared Spectrometer (CIRS; Flasar et al., 2004) have led to extensive characterization of the composition and thermal structure in the troposphere and stratosphere (e.g., Flasar et al., 2005; Fletcher et al., 2007; Fouchet et al., 2008; Guerlet et al., 2009; Sylvestre et al., 2015; Fletcher et al., 2016). Similarly, solar and stellar occultations from the Ultraviolet Imaging Spectrograph (UVIS; Esposito et al., 2004) have been used to characterize the mesosphere and thermosphere (Koskinen et al., 2013; 2015; Koskinen et al., 2016). In this work, we combine measurements from UVIS and CIRS to create empirical models of basic atmospheric structure in the middle and upper atmosphere at different latitudes and times.

Basic atmospheric structure consists of a temperature-pressure (T-P) profile and the altitudes corresponding to the pressure levels.

Observations from CIRS and UVIS constrain atmospheric structure at different altitudes. Regarding the temperature, UVIS occultations probe the thermosphere ($p \leq 0.1-0.01 \mu bar$) while infrared emissions by the collision-induced continuum and the v_4 band of CH₄ observed by CIRS probe the upper troposphere and stratosphere. In this work, we focus on the CIRS limb scans that are sensitive to the stratospheric temperature from about 1 μ bar to 20 mbar. In addition to temperature, atmospheric structure depends on the mean molecular weight, which in turn depends mostly on the relative abundances of H2 and He with a small contribution from CH4 and H. The constant mole fraction of CH₄ in the troposphere, based on far-IR emission data, is $(4.7 \pm 0.2) \times 10^{-3}$ (Fletcher et al., 2009). The abundance decreases rapidly with altitude around the homopause ($p \approx 0.01-1 \ \mu bar$) where the CH_4 density profile is probed by UVIS occultations. The abundances of H and He are uncertain and discussed below.

Atomic hydrogen is released by photochemistry. Koskinen et al. (2013) derived an upper limit of 5% for the volume mixing ratio of H in the thermosphere from Cassini occultations, which implies a negligible abundance in the lower atmosphere. This limiting value is consistent with the low abundances derived from Voyager solar occultations (Vervack and Moses, 2015). Thus the presence of H does not significantly affect our atmospheric structure models. Forward models of H Lyman α airglow data based on our atmospheric structure models can be used in future work to constrain

Corresponding author.

E-mail address: tommi@lpl.arizona.edu (T.T. Koskinen).

the abundance of H and inform photochemical models (e.g., Ben-Jaffel et al., 1995; Gustin et al., 2010). We note that our models are also an important reference for the interpretation of H_2 Lyman and Werner band emissions and H_3^+ infrared emissions that provide clues to the excitation state of H_2 , energy inputs and the influx of external material to the thermosphere (Shemansky et al., 2009; Gustin et al., 2010; O'Donoghue et al., 2013; Moore et al., 2015).

In contrast to H and CH₄, the abundance of helium in the lower atmosphere has a significant impact on atmospheric structure. Helium has no spectral features that can be directly detected by remote sensing and used to retrieve its abundance. In-situ measurements are only available for Jupiter where the Galileo probe measured a He/H₂ ratio of 0.157 \pm 0.003, corresponding to a mass fraction of $Y = 0.234 \pm 0.005$ (von Zahn and Hunten, 1996; von Zahn et al., 1998). This value falls below the protosolar mass fraction of Y = 0.27 (Asplund et al., 2009), implying a modest depletion of helium in the atmosphere due to the phase separation of helium and hydrogen in the interior (e.g., Hubbard et al., 1999). The relative enrichment of helium in the interior is believed to affect the structure and evolution of giant planets, providing clues to their formation. This makes the abundance of helium in the atmosphere a fundamental property of giant planets.

Contradicting results based on indirect measurements have led to considerable debate over the abundance of helium on Saturn. Conrath et al. (1984) obtained a relatively low He/H_2 ratio of 0.034 ± 0.024 , corresponding to a mass fraction of Y=0.01-0.11, by combining Voyager/IRIS infrared data with radio occultations. Their method is based on using the refractivity profile from radio occultations to derive density as a function of altitude in the lower atmosphere while infrared emission data probing the same location constrains the temperature. Thus the mean molecular weight, which depends on the abundance of helium, can be fitted to match both datasets simultaneously. A mass fraction of only about 0.06, however, would imply substantial depletion of helium in the envelope that is difficult to explain with models of thermal evolution for the planet. Based on such models, Hubbard et al. (1999) called for a reassessment of the uncertainties in the Voyager retrieval.

Conrath and Gautier (2000) found that the combined Voyager/IRIS and radio occultation retrieval underestimates the in-situ measurement of the helium abundance by the Galileo probe on Jupiter, due to systematic errors that are still not fully understood. As a result, they made another attempt to measure the helium abundance on Saturn by using the Voyager/IRIS data alone. This time, the retrieval was based on a subtle spectral signature of He-H₂ interactions in the collision-induced absorption by H₂ at the 200-600 cm⁻¹ wavenumber range. They found a revised He/H₂ ratio of 0.11-0.16, corresponding to a mass fraction of 0.18-0.25, in better agreement with evolutionary models. The new retrieval, however, is ill-posed in the sense that unique solutions cannot be obtained directly and small changes in the measurements can produce relatively large changes in the result. This has led to a persistent uncertainty on Saturn's helium abundance with possible values of the He/H_2 ratio usually taken to range from 0.03 to 0.16.

Our work provides new constraints on the abundance of helium based on the best-fit atmospheric structure models for several UVIS occultation locations and CIRS observations acquired in limb viewing geometry. In the well-mixed part of the atmosphere, both pressure and the partial pressure of H_2 decrease exponentially with altitude following a common scale height that depends on temperature and the mean molecular weight of the atmosphere. Given a T-P profile derived from the CIRS and UVIS data, we fit a forward model of the atmosphere to the H_2 density-altitude profile in the thermosphere to back out the mean molecular weight and the mixing ratio of helium in the lower atmosphere. In doing so, we use the 1 bar level from radio occultations and gravity

field measurements as an altitude reference (Anderson and Schubert, 2007). We note that the retrieval of T-P profiles depends on the assumed helium abundance but the effect of different abundances is small and instead the primary effect of changing the abundance of helium is to change the pressure level altitudes. The altitude offset is relatively small in the middle atmosphere but it grows with altitude towards the base of the thermosphere.

Indeed, the strength of our method lies in the fact that pressure in the thermosphere is many orders of magnitude below 1 bar and thus the cumulative effect of the mean molecular weight on the density level altitudes there is relatively large. Also, the UVIS stellar occultations do not suffer from any significant uncertainty in pointing and the line of sight altitudes are precisely known. The primary uncertainties in our models are due to a gap in temperature coverage in the mesosphere and the fact that the UVIS and CIRS observations do not generally coincide exactly in time and location. Our forward model also has to account for the transition from a well-mixed atmosphere to diffusive separation of constituents in the thermosphere based on the observed CH₄ profile. We quantify and mitigate the effect of these uncertainties by fitting many different observations that probe different times and locations.

We describe the relevant observations and their analysis in Section 2 where we also provide a detailed description of the empirical atmosphere structure model. In Section 3, we derive the best fit helium abundance and use our models at different occultation locations to derive mean values for the temperature and methane abundance in the upper atmosphere. We also explore the variations of temperature and the abundance of CH_4 with latitude and time. In Section 4, we compare our results with previous work and discuss their implications on the thermal structure and dynamics of the upper atmosphere. Section 5 provides our summary and conclusions.

2. Observations and data analysis

2.1. Cassini/UVIS stellar occultations

The stellar occultations that we use are observed simultaneously in the EUV (563-1182 Å) and FUV (1115-1912 Å) channels of the Cassini/UVIS instrument (McClintock et al., 1993; Esposito et al., 2004). We selected 32 occultations that probe the upper atmosphere at mid to low-latitudes from the spring of 2005 to the end of 2015 as the basis for our atmospheric models (see Table 1). We have analyzed the total of 39 occultations covering this time period but excluded two occultations probing high latitudes and five occultations of poor quality. We retrieve density profiles of CH_4 , C_2H_2 , C_2H_4 and C_2H_6 in the upper stratosphere and mesosphere from the data in the FUV channel. We detect evidence for the C₆H₆ ring molecule in 22 occultations. This adds four new occultations with such evidence to the previous detections by Koskinen et al. (2016). We use the data in the EUV channel to retrieve the H₂ density profile and temperature in the thermosphere. Fig. 1 shows the coverage of the UVIS occultations and relevant CIRS limb scans in time and planetographic latitude (ϕ_{pg}). Section 2.2 summarizes the analysis of the CIRS observations.

During stellar occultations, the signal spectrum of the star $S(\lambda_b, z_t)$ is observed along different lines of sight (LOS) through the atmosphere and divided by the unattenuated spectrum $S_0(\lambda_b)$ to obtain transmission as a function of tangent altitude z_t and wavelength band λ_b . Tangent altitude is measured along the local surface normal and it is the shortest distance between the LOS and the 'nearpoint' on the 1 bar surface. We calculate tangent altitudes by using SPICE kernels and the subroutines provided by the Navigation and Ancillary Information Facility (NAIF). We also calculate the planetocentric coordinates (radial distance and latitude) of

Download English Version:

https://daneshyari.com/en/article/8134216

Download Persian Version:

https://daneshyari.com/article/8134216

<u>Daneshyari.com</u>